Joule

CellPress
OPEN ACCESS

Report

ATP production from electricity with a new-to-nature electrobiological module

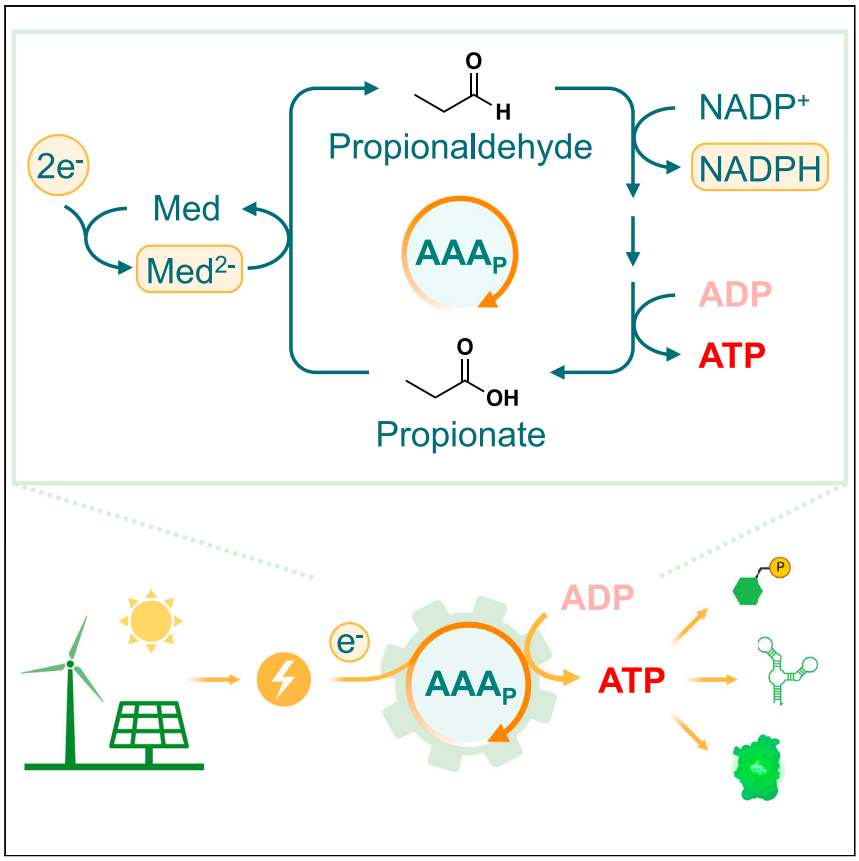

Electrification with renewables is key to a sustainable energy system. However, the direct use of electricity by biological systems is still limited. To interface the electrical and biological worlds, we designed a synthetic electrobiological module, the AAA cycle. The AAA cycle is a multi-step enzyme cascade that is able to produce the biological energy carrier ATP continuously from electricity. This allows for powering chemical reactions and more complex biological processes, including information processing and protein synthesis, with electrical energy.

Shanshan Luo, David Adam, Simone Giaveri, ..., Fabian Arndt, Johann Heider, Tobias J. Erb

shanshan.luo@mpi-marburg.mpg.de (S.L.)
toerb@mpi-marburg.mpg.de (T.J.E.)

Highlights

Synthetic biology approach to power biological systems directly from electricity

A synthetic enzyme cascade for converting electrical energy into ATP

Regeneration of ATP and other biological energy storage molecules from electricity

Electricity-driven information processing (transcription) and protein synthesis

Luo et al., Joule 7, 1745–1758
August 16, 2023
https://doi.org/10.1016/j.joule.2023.07.012

Joule

CellPress
OPEN ACCESS

Report

ATP production from electricity with a new-to-nature electrobiological module

Shanshan Luo,[1,*] David Adam,[1] Simone Giaveri,[1] Sebastian Barthel,[1] Stefano Cestellos-Blanco,[1,2,3] Dominik Hege,[4] Nicole Paczia,[5] Leonardo Castañeda-Losada,[6] Melanie Klose,[1] Fabian Arndt,[4] Johann Heider,[4] and Tobias J. Erb[1,7,8,*]

SUMMARY

Electricity is paramount to the technical world and plays an increasingly important role as a future energy carrier. Yet, it is not widely used to directly power biological systems. Here, we designed a new-to-nature electrobiological module, the acid/aldehyde ATP cycle (AAA cycle), for the direct conversion of electrical energy into ATP. The AAA cycle contains a minimum set of enzymes and does not require membrane-based charge separation. Realizing a propionate-based version of the AAA cycle, we demonstrate continuous, electricity-driven regeneration of ATP and other energy storage molecules from −0.6 V vs. SHE at 2.7 μmol cm^{-2} h^{-1} and faradaic efficiencies of up to 47%. Notably, the AAA cycle is compatible with complex cell-free systems, such as *in vitro* transcription/translation, powering the processing of biological information directly from electricity. This new link between the technical and biological worlds opens several possibilities for future applications in synthetic biology, electrobiotechnology, and bioelectrocatalysis.

INTRODUCTION

The transition to renewable energy systems is instrumental for achieving a carbon-neutral society. Electrification, especially when based on renewable energies, is a key element in reaching this goal and is expected to increase worldwide from 21% to 30% of the total energy consumption by 2030 (https://www.iea.org/reports/electrification). Despite the growing availability of electricity from renewables, one major challenge is the use and storage of electrical power, which currently amounts to ~3 terawatts (TW) per year (ca. 28,000 TWh, ca. 100 exajoule).[1,2] Several energy storage systems have been developed, with batteries being one of the most prominent technical storage solutions.

Even though biological systems are able to use and store more than 130 TW per year,[3] interfacing them directly with electricity has been explored only sparsely.[4,5] Current efforts to use (and store) electrical energy in biological systems mainly focus on the electricity-powered production of electron-carrying substrates, such as hydrogen, CO, formate, methanol, or acetate.[6–8] These electron carriers are subsequently metabolized and/or respired by microbial cells to conserve chemical energy.[9–13] Alternatively, electromicrobial systems have been developed in which microbial cells are directly powered with electricity.[14,15] However, all these cases represent examples for cell-based systems, which allocate a significant fraction of the energy for self-replication and often suffer from a mismatch between engineering and cellular objectives.[16]

CONTEXT & SCALE

Renewable electricity, as a clean energy carrier, can also be an energy source for biological systems. However, to directly power biological systems with electricity, electrical energy needs to be converted into ATP, the universal energy currency of life. Using synthetic biology, we designed a minimal "electrobiological module," the AAA cycle, that allows direct regeneration of ATP from electricity. The AAA cycle is a multi-step cascade of 3–4 enzymes that does not require any membranes and can be interfaced with many different applications. We show how ATP and other biological energy storage molecules can be produced continuously at −0.6 V and further demonstrate that more complex biological processes, such as RNA and protein synthesis from DNA, can also be powered by electricity. Our synthetic electrobiological module provides a direct interface between electricity and biology, and opens up new avenues for electricity-driven biological systems for a sustainable future.

An up-and-coming field with great perspective to overcome these limitations is cell-free or *in vitro* biological systems. Although these systems are increasingly used in academia and industry, a major drawback is their requirement for external chemical energy. To directly power cell-free systems with electricity, there is a need to convert electrical energy into biochemical energy, specifically reducing power (e.g., NAD(P)H and ferredoxin) and adenosine triphosphate (ATP), the universal energy currency of the cell. Although methods for producing redox cofactors from electricity have been established,[17,18] the conversion of electric energy into ATP has yet to be demonstrated.

In cells, ATP is synthesized through a rather complicated process involving several membrane-bound redox protein complexes. Electrons are transferred along different redox centers, creating a proton motive force across the membrane, which is subsequently harvested for ATP synthesis (Figure 1A). However, using this sophisticated system *in vitro* is challenging because it requires the stable assembly of multiple enzyme complexes in the correct orientation and stoichiometry within a membrane. Moreover, introducing these membrane systems to cell-free systems inevitably increases complexity and decreases the robustness of the *in vitro* system. Overall, the complex biochemistry of naturally evolved membrane-based systems or comparable vesicle-based derivatives[19–22] has restricted the use of external electricity to power cell-free and/or *in vitro* systems.

To overcome these challenges, we sought to design an interface between electricity and biological systems that would provide a simpler way from electrical energy into ATP. Specifically, we aimed to realize a new-to-nature electrobiological module that (1) comprises a minimal set of biological components, (2) does not involve membrane-bound charge separation, and (3) can be coupled to other *in vitro* modules, providing a direct way to power complex cell-free biological systems with electricity (Figure 1C).

RESULTS

Design of the AAA cycle

To realize a minimal electrobiological module for the continuous production of ATP from electricity, we first looked into the possible ways to generate ATP from adenosine diphosphate (ADP) and inorganic phosphate (Pi) enzymatically. Besides membrane-bound ATP synthase, several membrane-independent enzyme systems have been described that convert the energy stored in mixed phosphoanhydrides (e.g., acetate kinase [AckA] and 3-phosphoglycerate kinase), *enol* phosphates (pyruvate kinase), or thioesters (guanosine diphosphate [GDP]-forming succinyl-coenzyme A [CoA] synthetase and ADP-forming 4-hydoxybutyryl-CoA synthetase) into ATP under release of the free acids, making them prime targets for the ATP-forming step.[23]

To employ these ATP-generating reactions in an electrobiological module, the free acids need to be recycled back to the substrates through electrochemical activation. Several enzymes have been described that use low-potential electrons to directly reduce free acids into their corresponding aldehydes.[24–27] The energy stored in these aldehydes can be subsequently harnessed to oxidatively generate phosphoacid anhydrides, either directly or via concomitant CoA thioester formation and subsequent transfer of the phospho-group. Combined together, these reactions form a 3–4 reaction cycle, in which low-potential electrons are used to drive the formation of ATP (as well as NAD(P)H) through an acid/aldehyde redox couple, which we termed the acid/aldehyde ATP cycle (AAA cycle, Figure 1B).

[1]Department of Biochemistry and Synthetic Metabolism, Max Planck Institute for Terrestrial Microbiology, 35043 Marburg, Germany

[2]Department of Chemical Engineering, Stanford University, Stanford, CA 94305, USA

[3]Green Talents Program, German Federal Ministry of Education and Research, 53175 Bonn, Germany

[4]Microbiology, Philipps University of Marburg, 35037 Marburg, Germany

[5]Metabolomics Facility, Max Planck Institute for Terrestrial Microbiology, 35043 Marburg, Germany

[6]Fraunhofer Institute for Interfacial Engineering and Biotechnology IGB, Bioinspired Chemistry, 94315 Straubing, Germany

[7]Center for Synthetic Microbiology (SYNMIKRO), 35037 Marburg, Germany

[8]Lead contact

*Correspondence:
shanshan.luo@mpi-marburg.mpg.de (S.L.),
toerb@mpi-marburg.mpg.de (T.J.E.)

https://doi.org/10.1016/j.joule.2023.07.012

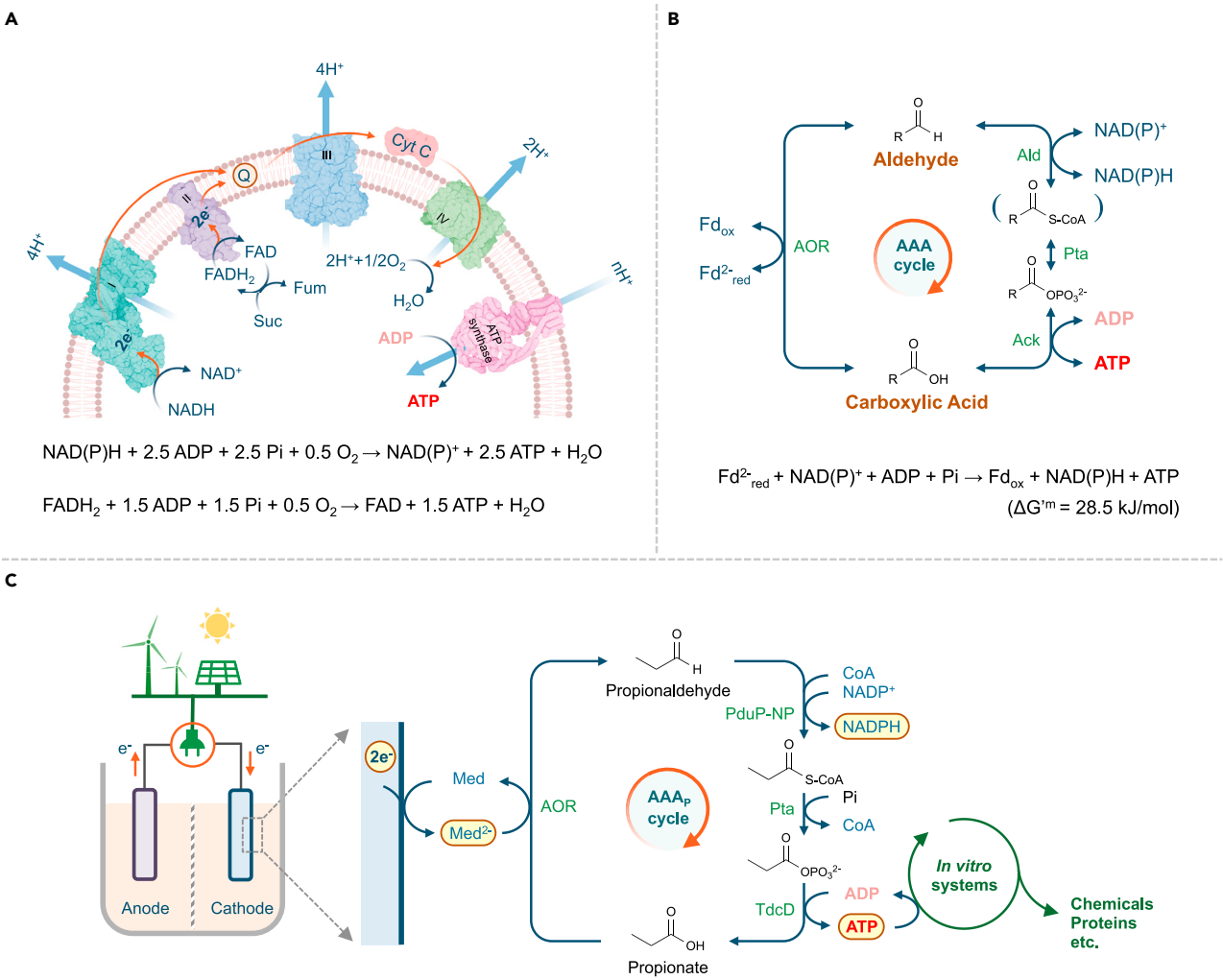

Figure 1. The AAA cycle: a minimal electrobiological module

(A) ATP synthesis through oxidative phosphorylation, electrons from NADH, and $FADH_2$ pass to O_2 through a series of redox centers in the electron transport chain (ETC), going from a higher energy level to a lower energy level, creating a proton gradient across the membrane. The electrochemical energy stored in this gradient then drives the synthesis of ATP as protons flow back through ATP synthase. In the scheme, a phosphate/oxygen (P/O) ratio of 2.5 for NAD(P)H and 1.5 for $FADH_2$ is assumed.

(B) ATP synthesis through the AAA cycle developed in this work. Enzymatic conversion of an aldehyde to a carboxylic acid can either produce reduced ferredoxin, or NAD(P)H and ATP. Coupling the ferredoxin- and ATP/NAD(P)H-dependent branches allows us to draft a cycle in which a carboxylic acid is first reduced to an aldehyde using reduced ferredoxin as reducing equivalent and then recycled back while generating NAD(P)H and ATP. The net reaction is converting an electron carrier of higher energy, reduced ferredoxin, to lower-energy reducing power, NAD(P)H, while using the energy difference to produce ATP.

(C) Technical implementation of the AAA cycle. A propionate-based AAA cycle converts electricity into ATP, which can power various *in vitro* systems, as shown in this work. Suc, succinate; Fum, fumarate; $Fd^{2-}{}_{red}$, reduced ferredoxin; Fd_{ox}, oxidized ferredoxin; Ald, CoA-acylating aldehyde dehydrogenase; Ack, acid kinase.

Realization of the AAA cycle

To realize the AAA cycle, we first focused on identifying an enzyme candidate for the reduction of non-activated carboxylic acids into their corresponding aldehydes, which is thermodynamically challenging due to the very low redox potential of acid/aldehyde couples (E'° = −580 mV). Ferredoxin-dependent aldehyde oxidoreductases (AORs) have been shown to catalyze this reaction *in vivo* with reduced ferredoxin ($Fd^{2-}{}_{red}$)[28,29] and *in vitro* with low-potential electron carriers such as reduced tetramethyl viologen (TMV) (E'° = −536 mV),[30] Ti (III) citrate

(E'° = −800 mV),[31] or Eu (II)-EGTA (E'° = −1,100 mV).[32] AORs are classified into several branches, including formaldehyde ferredoxin oxidoreductase (FOR), glyceraldehyde-3-phosphate ferredoxin oxidoreductase (GAPOR), and broad-substrate range aldehyde ferredoxin oxidoreductase (WORs or bona fide AORs). Thus, various AAA cycles can be designed based on different AORs (Figure S1).

Recently, a tungsten-containing AOR from the mesophilic betaproteobacterium *Aromatoleum aromaticum* EbN1 (AOR_{Aa}) has been isolated and characterized in detail.[31] This enzyme catalyzes the oxidation of different aldehydes, including benzaldehyde, acetaldehyde, and propionaldehyde, with either benzyl viologen (BV) or NAD^+ as electron acceptors. Compared with related enzymes from other microorganisms, AOR_{Aa} is highly active at ambient temperatures, remarkably stable after exposure to air (>1 h half-life), and can be conveniently purified from a homologous expression system.[31,32] Based on the favorable characteristics and availability of AOR_{Aa}, we decided to use this protein to realize an AAA cycle with acetate or propionate. To catalyze the acid reduction reaction of AOR_{Aa}, we sought to use hexamethyl viologen (HMV, E'° = −610 mV) as a soluble electron carrier and kinetically/thermodynamically favorable conditions, including a low pH (pH = 6), high substrate concentration (60 mM acetate or propionate), as well as constant removal of the aldehyde product with phenylhydrazine. Under these conditions, AOR_{Aa} catalyzed the reduction of acetate and propionate into the corresponding aldehydes (demonstrated as their phenylhydrazones; Figures 2A and S2) at 72 ± 3 and 57 ± 3 mU/mg, respectively (Figure S3).

Next, we aimed at coupling AOR_{Aa} with a CoA-acylating aldehyde dehydrogenase to further convert the aldehydes into their corresponding CoA esters. Note that AOR_{Aa} accepts NAD^+ as an electron acceptor but not $NADP^+$.[31] To avoid direct transfer of electrons from reduced HMV onto NAD^+ by AOR_{Aa}, which would shortcut the AAA cycle, we sought to employ an NADPH-dependent enzyme. We used a CoA-acylating propionaldehyde dehydrogenase (PduP-NP) from *Rhodopseudomonas palustris* BisB18 that was recently engineered to accept $NADP^+$ as an electron acceptor.[33,34] Kinetic characterization of PduP-NP demonstrated that the enzyme showed better catalytic properties for propionaldehyde (K_M = 0.77 ± 0.21 mM, V_{max} = 9.8 ± 1.1 U/mg) compared with acetaldehyde (K_M = 2.0 ± 0.54 mM and V_{max} = 2.8 ± 0.35 U/mg) (Figure S4). We thus decided to realize the AAA cycle based on propionate (AAA_P cycle).

When we coupled AOR_{Aa} and PduP-NP, we could demonstrate the formation of propionyl-CoA from propionate, using liquid chromatography-mass spectrometry (LC-MS). Adding pyruvate and lactate dehydrogenase (Ldh) to recycle NADPH further improved the yield (Figure S5). To further convert propionyl-CoA into propionylphosphate, we decided to use phosphate acetyltransferase (Pta) from *Escherichia coli*. For the ATP production step (i.e., converting propionylphosphate into propionate), we tested AckA and propionate kinase (TdcD) from *E. coli* and chose TdcD because of its favorable kinetic parameters with propionylphosphate (Figure S6).

With all enzymes for the AAA_P cycle at hand, we aimed at assembling the complete cycle. We first verified that the PduP-NP, Pta, and TdcD cascade produced ATP from propionaldehyde under the working conditions of AOR_{Aa} (i.e., pH = 6 in the presence of 60 mM propionate; Figure 2B). We then reconstructed the full cycle with AOR_{Aa}, used Ti(III)-reduced HMV as an electron donor, and added 60 mM propionate to start the cycle. Initial tests showed that the negative control without propionate also produced ATP, which we could trace back to myokinase contamination (Figure S7). Increasing the purity of protein preparations by additional size exclusion

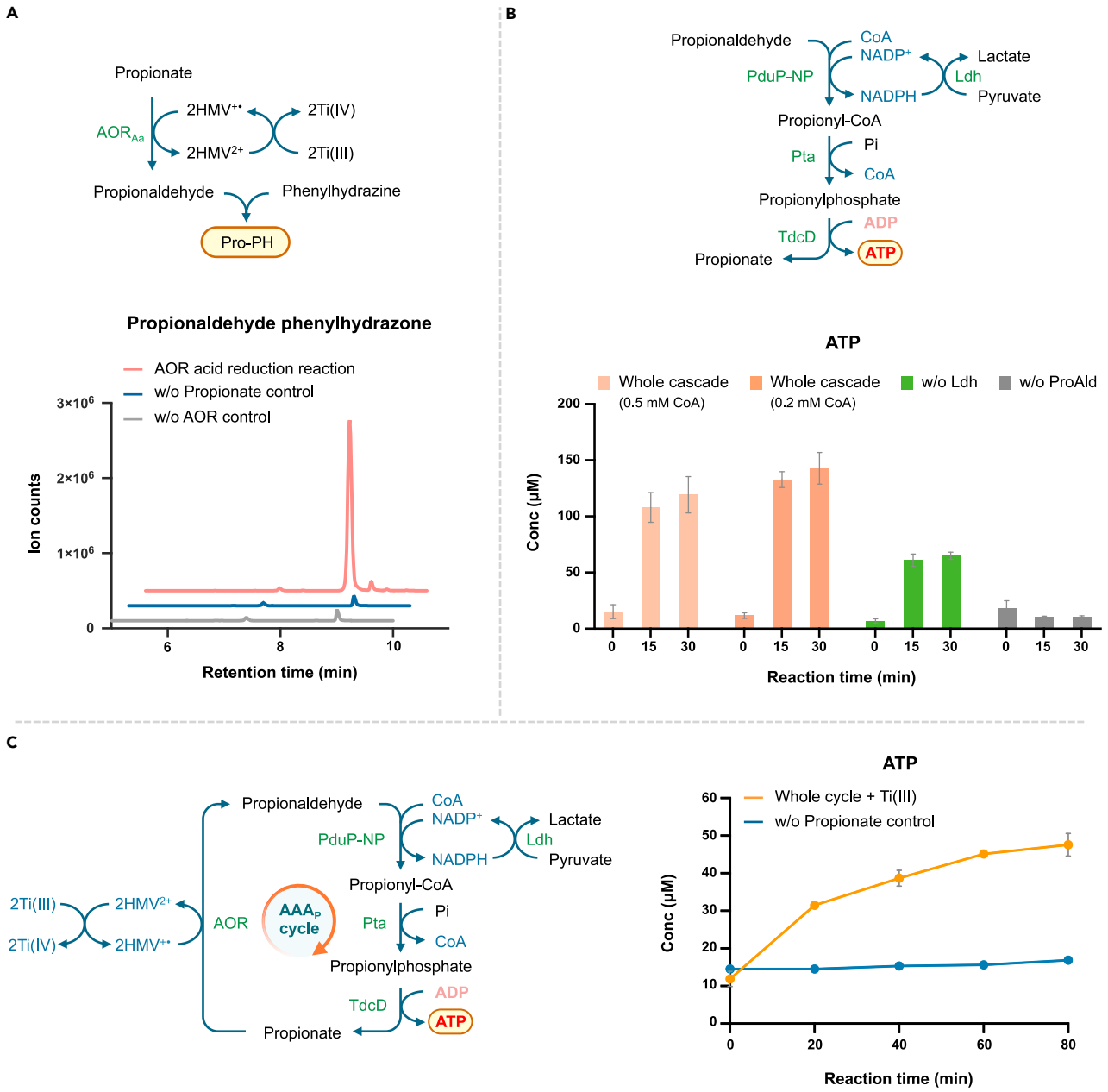

Figure 2. Demonstration of the AAA$_P$ cycle

(A) Verification of propionate reduction reaction of AOR$_{Aa}$ with LC-MS. HMV is reduced by Ti(III)-citrate to serve as an electron donor. Phenylhydrazine is added to drain away acetaldehyde. Reaction mixture in the absence of AOR$_{Aa}$ or propionate is used as the negative control.

(B) ATP production of the PduP-NP, Pta, and TdcD cascade under the working conditions of AOR$_{Aa}$. Pyruvate and Ldh were added for NADPH recycling. As shown, the cascade produced ATP from propionaldehyde under the working conditions of AOR$_{Aa}$ (i.e., pH = 6 with 60 mM propionate present), and recycling NADPH increased the yield.

(C) ATP production of the AAA$_P$ cycle powered by Ti(III) reduced HMV. Shown are the dynamics of ATP of the AAA$_P$ cycle over 80 min. The data in (B) and (C) represent mean ± SD (standard deviation) obtained in triplicate experiments (n = 3).

chromatography together with the addition of myokinase inhibitor, P1,P5-di(adenosine-5′)pentaphosphate (AP5A), suppressed background ATP formation in the controls. Under these optimized conditions, the AAA$_P$ cycle produced about 30 μM ATP in 80 min from Ti(III)-reduced HMV (Figure 2C).

Coupling of the AAA cycle with electricity

Having established the AAA_P cycle with reduced HMV, we aimed at coupling it to an electrochemical cell to directly power ATP formation from electricity. In our initial setup, all three electrodes (glassy carbon working, platinum counter, and Ag/AgCl reference electrode) of the electrochemical cell were placed in a single compartment. Although HMV was readily reduced and oxidized at the working electrode (Figure S8), the purple color characteristic of reduced HMV quickly disappeared after turning off electricity, indicating that the HMV reduced by electricity was not stable. Moreover, we also observed that the three-electrode setup negatively affected the AOR reaction (Figure S9). We therefore assumed that the counter electrode produced oxygen and/or reactive oxygen species (ROS) from water splitting, which would be detrimental for both reduced HMV and AOR. Therefore, we switched to an H-type cell, a two-compartment electrochemical cell with a proton-conducting Nafion membrane, to physically separate the cathodic and anodic compartments. With this setup, reduced HMV was functionally stable (Figure S10) and could be used as a mediator to power the production of 57 μM ATP in 45 min (Figure S11) in a discontinuous fashion (i.e., when the AAA_P cycle was subsequently added to the reaction mixture).

We next aimed at a continuous operation of the AAA_P cycle in the two-compartment system (Figure 3A). Initial experiments demonstrated that continuous ATP production was indeed possible and directly depended on the current applied (Figure S12). However, we noticed that reduced HMV could directly reduce $NADP^+$ at low rates that increased with the concentration of reduced HMV (Figure S13). In the absence of HMV, no reduction of $NADP^+$ (e.g., on the cathode) was observed (Figure S14). Cyclic voltammetry (CV) of HMV in the presence of different reagents of the AAA_P cycle (Figure S15) showed no significant background activity of HMV with other reaction components, indicating that reduced HMV only reacted with $NADP^+$. To avoid the accumulation of reduced HMV, we limited its production by operating the system between −0.57 and −0.53 V vs. standard hydrogen electrode (SHE). Under these conditions, we observed a current response of −0.51 to −0.14 mA/cm^2 (1.3–0.37 μmol electrons h^{-1}) (Figure S16), and the reaction mixture showed a very light purple color (at least over the first 2 h), indicating low steady-state concentrations of reduced HMV in the system.

After adjusting the steady-state concentrations of reduced HMV, we run the AAA_P cycle, using 0.3 mg/mL total enzymes (including the four AAA_P enzymes, as well as Ldh for NADPH recycling) and 60 mM propionate as the starting substrate. With this setup, we observed a faradaic efficiency (FE) for HMV reduction of about 70%–80% (Figure S17) and achieved continuous ATP production with up to 165 μM ATP produced in 5 h, reaching a yield of 17%. The steady-state (first hour) production rate was 1.03 μmol cm^{-2} h^{-1} at a total FE of 22% for ATP production (not counting any other reduced intermediates in the system; Figure 3B).

Application of the AAA cycle for energy and information storage

Having demonstrated the direct production of ATP from electricity with the AAA_P cycle, we sought to couple our minimal electrobiological module to different *in vitro* systems. We first coupled the AAA_P cycle to hexokinase (HK) for *in situ* production of glucose 6-phosphate (G6P). G6P is used as a redox and energy carrier for different biocatalytic systems[35] and is an important building block for energy storage in biological molecules, such as starch or glycogen. In our coupled system, about 400 μM G6P was produced in 4 h corresponding to a yield of 20%. The steady-state (first hour) production rate was 2.71 μmol cm^{-2} h^{-1} at 47% overall FE (Figure 3C). This

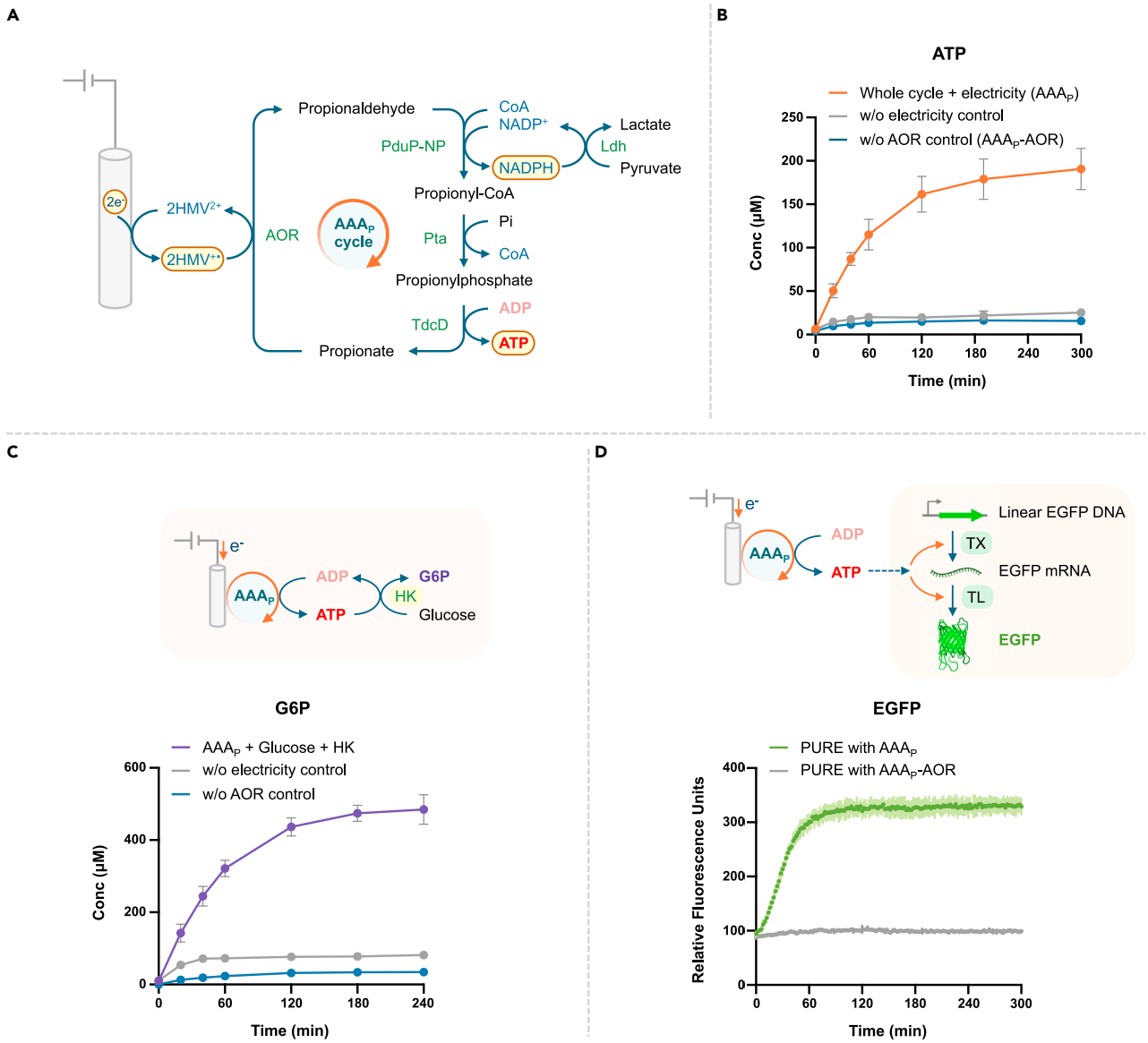

Figure 3. Electricity-driven ATP production from the AAA_P cycle and its applications

(A) Scheme of the AAA_P cycle producing ATP from electricity. In this cycle, AOR first converts propionate to propionaldehyde using HMV reduced by electricity. Propionaldehyde is further converted into propionate through three enzymatic steps, generating NADPH and ATP. Pyruvate and Ldh recycle NADPH to push the equilibrium toward the ATP-producing direction.

(B) ATP production of the AAA_P cycle over time, driven by electricity. The starting composition of the full cycle includes five enzymes (AOR, PduP-NP, Pta, TdcD, and Ldh), HMV, cofactors (CoA, $NADP^+$, and ADP), propionate, pyruvate, and AP5A. Omitting AOR or applied electricity from the system did not result in ATP production and served as negative controls. ATP concentrations were quantified by the luciferin-luciferase assay. The same samples were also quantified with LC-MS (see Figure S18 for the results).

(C) Coupling of electricity-produced ATP with G6P production from glucose. G6P was continuously produced from glucose and electricity when glucose and hexokinase (HK) were coupled with the AAA_P cycle. Omitting AOR or electricity from the system abolished G6P production. 1 mM ADP was initially introduced.

(D) Coupling of electricity-produced ATP with *in vitro* transcription (TX) and translation (TL). Shown is the fluorescence signal resulting from TX-TL of EGFP in a custom-prepared PURE system lacking ATP and energy-regenerating enzymes. The green curve is obtained by supplementing the PURE system with the full AAA_P cycle, after applying electricity for 5 h as sole source of ATP for performing TX-TL. In the negative control (gray curve), the PURE system was fed with an AAA_P cycle setup lacking the AOR enzyme, after applying electricity for 5 h. The data represent mean ± SD (standard deviation) obtained in triplicate experiments (n = 3) except for the without (w/o) AOR controls in (B) and (C) (n = 1).

indicated that coupling ATP production to downstream molecules (G6P) creates sinks that increase FEs.

Next, we aimed at powering more complex *in vitro* systems with our electrobiological module. One of the most fundamental processes in biology is information processing, in particular transcription (TX) and translation (TL) of nucleic acids. To demonstrate AAA_P cycle-powered TX, we used a modified RNA Output Sensor Activated by Ligand Induction (ROSALIND) platform.[36] In this TX system, a fluorogenic dye-binding RNA aptamer (3WJdB, "Broccoli") is expressed by T7 RNA polymerase under consumption of nucleotide triphosphates including ATP (Figure S19A). We run the AAA_P cycle for 5 h and added the reaction mixture into above TX system (lacking ATP) at a 1:10 dilution to detect a visible RNA output corresponding to about 20 μM ATP (Figure S19B). These results demonstrated that the ATP produced by the AAA_P cycle is incorporated into RNA, successfully linking biological information processing with electricity.

In the next step, we wanted to power both, TX-TL, with our electrobiological module to demonstrate the electrification of protein production from DNA templates. To establish such a system, we made use of a custom-prepared cell-free TX-TL system that lacks ATP and all enzymes for ATP regeneration (customized PUREfrex). We first optimized the system to detect the production of an enhanced green fluorescent protein (EGFP) or a luciferase (NanoLuc) from a DNA template, starting with ATP concentrations as low as 80 μM and ADP/ATP ratios as high as 4:1. We then run the AAA_P cycle for 5 h with electricity and transferred the reaction mixture in a 2:5 ratio into the PUREfrex system to produce either EGFP (Figure 3D) or NanoLuc luciferase (Figure S20). These experiments demonstrated the successful powering of *in vitro* protein production from electrically generated ATP serving as an mRNA monomer, as well as an energy source. Together, these experiments showed that one of the core processes of biological systems can, in principle, be directly powered by electricity.

DISCUSSION

In summary, we developed a new-to-nature module for the conversion of electricity into ATP, the universal energy currency of life. Our approach represents a fundamentally different strategy compared with recent efforts, which used electricity to facilitate the production of ATP from organic compounds but did not power ATP formation directly from electricity.[37]

Our electrobiological module, the AAA_P cycle, consists of only four enzyme components, does not require membrane-based charge separation, and can be coupled to different *in vitro* processes. Compared with natural or reconstructed membrane-based systems, the AAA_P cycle allows the direct use of electrical energy for biological processes, such as catalytic conversions and information processing and its further storage in biological molecules (such as G6P, nucleic acids, or proteins). When coupled to downstream processes, the AAA_P cycle shows a FE of up to 47% even without extensive optimization. Improving FE further will directly improve the overall efficiency of the AAA_P cycle. One factor limiting FE is the instability of reduced HMV and its spontaneous reduction of $NADP^+$. This limitation could be overcome by switching to other electron mediators and/or by more carefully controlling their concentrations in the electrochemical system.

In our current setup, we produced 0.2–0.4 mM ATP from 1 mM ADP. This yield is likely thermodynamically limited by the high concentration of propionate in the

system, which inevitably limited the conversion from propionaldehyde to propionate through PduP-NP, Pta, and TdcD (and in particular, the release of propionate from propionylphosphate). At the same time, high propionate concentrations are required to boost the propionate reduction reaction of AOR. Note that AORs have high K_M for carboxylic acids probably because only the protonated acid can bind to the enzyme and act as the substrate.[38] Because the AOR reaction with reduced HMV itself is not thermodynamically limited (E'° (acid/aldehyde) = −580 mV vs. E'° ($HMV^{2+}/HMV^{+\bullet}$) = −610 mV, resulting in a $\Delta G'^{\circ}$ = −5.79 kJ/mol), improving the kinetic parameters of the enzyme (e.g., lowering its K_M for propionate) has the potential to improve product yields of the AAA_P cycle.

The AAA_P cycle shows an estimated energy efficiency of 17% (Note S1) and is currently limited by FE losses and relatively low NADPH/$NADP^+$ and ATP/ADP ratios. However, our synthetic module still compares favorably with naturally evolved solutions. In nature, the bifurcating enzyme, ferredoxin:NAD^+ reductase (Rnf), couples the transfer of two electrons onto $NADP^+$ with proton or ion pumping across a membrane, which allows the cells to create 0.5 ATP.[39,40] By contrast, our electrobiological module allows the direct production of 1 ATP from transferring two electrons onto $NADP^+$ without a membrane. This is achieved by using the artificial mediator HMV as the electron donor, which shifts the thermodynamics of the AAA_P cycle from $\Delta G'^{m}$ = 28.5 kJ/mol (Fd^{2-}_{red} + $NAD(P)^+$ + ADP + Pi → Fd_{ox} + NAD(P)H + ATP) to −9.7 kJ/mol ($2HMV^{+\bullet}$ + $NAD(P)^+$ + ADP + Pi → $2HMV^{2+}$ + NAD(P)H + ATP), showcasing the potential of synthetic biological systems for expanding the natural solution space by new designs.

Overall, the AAA_P cycle provides a direct interface between electrical and biological systems, which might lay the foundation for different applications in bio(electro) catalysis, biotechnology, and synthetic biology in the future. Using electricity directly for storing energy and information in (synthetic) biological systems will open new ways to link the technical and natural worlds.

EXPERIMENTAL PROCEDURES

Resource availability

Lead contact

Further information and requests for resources should be directed to the lead contact, Dr. Tobias J. Erb (toerb@mpi-marburg.mpg.de).

Materials availability

Strains and plasmids used in this study are available upon request from the lead contact. This study did not generate new unique chemicals.

Data and code availability

The datasets generated in this study are available from the lead contact on reasonable request.

Synthesis of hexamethylviologen chloride (4,4′-Bipyridinium, 1,1′,2,2′,6,6′-hexamethyl-, chloride)

Tetramethyl bipyridine (0.8 g, 3.8 mmol) was slowly heated in dimethyl sulfate (6 mL) to 110°C. After 1 h, the cooled solution was poured into Et_2O (20 mL) to precipitate the viologen product as a $MeSO_4^-$ salt that was filtered and washed with Et_2O. The $MeSO_4^-$ counterion was exchanged in two steps into Cl^-. First, the $MeSO_4^-$ counterion was exchanged to PF_6^- by adding portion-wise NH_4PF_6 (6.2 g, 38 mmol) to

a solution of the $MeSO_4^-$ viologen in water (10 mL). The reaction mixture was stirred at room temperature overnight. The PF_6^- viologen product was filtered, washed with cold water, and dried under a high vacuum. Finally, the counterion was exchanged into Cl^- by adding tetrabutylammonium chloride (10.6 g, 38 mmol) to a solution of the PF_6^- viologen in acetonitrile (ACN) (50 mL). The mixture was stirred overnight at room temperature. The product was filtered, washed with cold ACN, and dried under a high vacuum. The viologen chloride was obtained with 41% yield (0.49 g, 1.6 mmol). ^{1}H NMR (400 MHz, D_2O) δ/ppm: 8.18 (s, 4H, aromatic), 4.18 (s, 6H, N-CH_3), 2.93 (s, 12H, C-CH_3) (Figure S21). ^{13}C NMR (101 MHz, D_2O) δ/ppm: 157.32, 148.75, 125.45, 40.28, and 21.50 (Figure S22). The redox potential of the viologen derivative was measured using a three-electrode setup (glassy carbon working electrode, platinum counter electrode, and Ag/AgCl 3.5 M reference electrode) in 100 mM phosphate buffer pH 6. A midpoint potential of −610 mV vs. SHE ($E_{p,a}$ = −582, $E_{p,c}$ = −637 mV vs. SHE, average values based on measurements at various scan rates) was found for the single electron reduction step of the viologen dication into the radical cation state (Figure S8). The reaction scheme for this synthesis is:

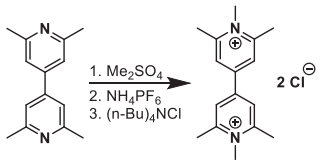

Plasmid construction

See supplemental experimental procedures for details. Plasmids are listed in Table S1. Primers used are listed in Table S2.

Protein expression and purification

See supplemental experimental procedures for details. See Figure S23 for the SDS-PAGE of all purified proteins.

Assay of the PduP-NP, Pta, and TdcD cascade

The PduP-NP, Pta, and TdcD cascade was assayed aerobically under the working conditions of AOR_{Aa}. The assay was performed in a 50 μL reaction mixture containing 100 mM phosphate buffer pH 6, 5 mM $MgCl_2$, 0.2 mM propionaldehyde, 1 mM $NADP^+$, 1 mM ADP, 0.2 mM or 0.5 mM CoA, 0.5 mM pyruvate, 60 mM propionate, 0.2 mM AP5A, 1.8 μg PduP-NP, 0.7 μg Pta, 0.4 μg TdcD, and 0.9 μg Ldh. The reaction was started with the addition of propionaldehyde. A reaction mixture without adding propionaldehyde was used as the negative control. A reaction mixture containing everything (with 0.5 mM CoA) except Ldh was set up to check the effect of NADPH recycling. Samples (10 μL) were withdrawn, mixed with 40 μL AXP internal standard mixture (2 μM AMP-$^{15}N_5$, 2 μM ADP-$^{15}N_5$, and 2 μM ATP-$^{13}C_{10}$ in H_2O), quenched with 3% formic acid, and analyzed for AXPs with LC-MS/MS using the method described in supplemental experimental procedures.

Assay of the AAA_P cycle powered with Ti(III) reduced HMV

The assay was performed anaerobically in a 50 μL reaction mixture containing 100 mM phosphate buffer pH 6, 5 mM $MgCl_2$, 5 mM HMV, 0.6 mM Ti(III)-citrate, 1 mM $NADP^+$, 1 mM ADP, 0.25 mM CoA, 0.5 mM pyruvate, 60 mM propionate, 0.2 mM AP5A, 8.7 μg AOR_{Aa}, 2.1 μg PduP-NP, 0.7 μg Pta, 0.4 μg TdcD, and 0.8 μg Ldh. Ti(III)-citrate was first added into phosphate buffer containing HMV to produce reduced HMV. Subsequently, other components were added to the

reduced HMV containing buffer. The reaction was started with the addition of propionate. A reaction mixture without adding propionate was used as the negative control. Samples (10 μL) were withdrawn, mixed with 40 μL AXP internal standard mixture (2 μM AMP-$^{15}N_5$, 2 μM ADP-$^{15}N_5$, and 2 μM ATP-$^{13}C_{10}$ in H_2O), quenched with 3% formic acid, and analyzed for AXPs with LC-MS/MS using the method described in supplemental experimental procedures.

Setup of electrochemical experiments

All electrochemical experiments were performed using an EmStatblue (Palmsense) potentiostat. A three-electrode setup was employed using a glassy carbon electrode as the working electrode, a platinum as the counter electrode, and an Ag/AgCl (3.5 M KCl) (eday, ETO72) as the reference electrode. All potentials were reported vs. the SHE using E(SHE) = E(Ag/AgCl 3.5 M) + 205 mV. The glassy carbon electrodes with a diameter of 3 mm were polished using alumina powder following the standard protocols. The electrochemical experiments were run under oxygen-free conditions inside a glovebox (Vinyl Glove Box, COY Lab Products). Electrochemical experiments were carried out in a single compartment or in a two-compartment setup separated by a Nafion membrane (Nafion N117, Ion Power).

Assay of electricity-powered AAA_P cycle

The assay was performed anaerobically in an 800 μL reaction mixture containing 100 mM phosphate buffer pH 6, 5 mM HMV, 5 mM $MgCl_2$, 1 mM $NADP^+$, 1 mM ADP, 0.25 mM CoA, 0.5 mM pyruvate, 60 mM propionate, 0.2 mM AP5A, 177.8 μg AOR_{Aa}, 27.6 μg PduP-NP, 10.0 μg Pta, 6.0 μg TdcD, and 11.8 μg Ldh. Except for AOR_{Aa}, other enzymes were prepared aerobically and contained oxygen. To guarantee an anaerobic environment before adding AOR_{Aa}, a small amount of reduced HMV was first produced to scavenge oxygen. To do so, the HMV containing phosphate buffer was reduced for 330 s at −0.56 V vs. SHE with stirring (at 500 rpm) directly under the working electrode. The current was around −0.4 mA/cm^2 under this condition. Subsequently, other components were added to a final 900 μL volume. Then, a 100 μL mixture was taken out to react without electricity as the negative control. The rest of the 800 μL reaction mixture was placed in a two-compartment electrochemical cell with a glassy carbon electrode (0.07 cm^2 area), and reduced for 5 h at potentials between −0.57 and −0.53 V vs. SHE. The potential was adjusted according to the color of the reaction mixture to keep the reduced HMV (purple color) concentration low (see Figure S16 for details). A reaction mixture containing everything except AOR_{Aa} was applied electricity with the same potentials for 5 h as another negative control. Samples (17 μL) were withdrawn at different time points. 10 μL sample was mixed with 40 μL AXP internal standard mixture (2 μM AMP-$^{15}N_5$, 2 μM ADP-$^{15}N_5$, and 2 μM ATP-$^{13}C_{10}$ in H_2O), quenched with 3% formic acid, and analyzed for AXPs with LC-MS/MS using the method described in supplemental experimental procedures. The 2 μL sample was mixed with 198 μL water and analyzed for ATP with the luciferin-luciferase assay using the ATP Bioluminescence Assay Kit CLS II and following the manufacturer's protocol.

The FE of ATP production, FE_{ATP}, was calculated based on the following equation:

$$FE_{ATP} = \frac{(C_{ATP60m} \times V_{60m} + (C_{ATP20m} + C_{ATP40m}) \times V_s) \times 2 \times F}{\int i\,(A)\,dt}$$

Here C_{ATP20m}, C_{ATP40m}, and C_{ATP60m} (mol L^{-1}) are the ATP concentration (quantified with the luciferin-luciferase assay) in the reaction mixture subtract the ATP concentration in without electricity control at times 20, 40, and 60 min, respectively. V_{60m} (L) is the volume of the reaction mixture at time 60 min, V_s is the sample volume

(17 μL), F (C mol^{-1}) is the Faraday constant, and $\int i\,(A)\,dt$ is the amount of electrons passed through the working electrode in the first hour.

In vitro TX-TL assay

Energy solution preparation

The following solutions were prepared. SolutionA(-Salts-tRNAs-amino acids [AAs]-ATP) (2 mL):creatine phosphate (147.06 mM), folinic acid (0.15 mM), spermidine (14.71 mM), DTT (7.4 mM), guanosine triphosphate (GTP) (14.71 mM), cytidine triphosphate (CTP) (7.4 mM), uridine triphosphate (UTP) (7.4 mM), and HEPES (pH 7.6, 367.65 mM). Salts solution (2 mL): magnesium acetate (184.38 mM), and potassium glutamate (1.563 M). tRNAs solution (200 μL): tRNAs (560 A_{260} mL^{-1}). tRNAs were quantified by using UV absorption A_{260} in Thermo Scientific NanoDrop 2000 spectrophotometer. AAs solution (4 mL): 20 proteinogenic AAs (3 mM). The four solutions were combined in a 50 μL reaction, by mixing 6.8/3.2/5/5 v/v/v/v solutionA(-Salts-tRNAs-AAs-ATP):salts solution:tRNAs solution:AAs solution, in order to get the desired concentrations, adapted from Ueda and coworkers[41]: creatine phosphate (20 mM), folinic acid (0.02 mM), spermidine (2 mM), DTT (1 mM), GTP (2 mM), CTP (1 mM), UTP (1 mM), HEPES (pH 7.6, 50 mM), magnesium acetate (11.8 mM), potassium glutamate (100 mM), tRNAs (56 A_{260} mL^{-1}), and AAs (0.3 mM).

Coupling the AAA_P cycle with TX-TL for EGFP production

6.8 μL of solutionA(-Salts-tRNAs-AAs-ATP), 3.2 μL of salts solution, 5 μL of tRNAs solution, 5 μL of AAs solution, 2.5 μL custom PURExpress Solution II Δ(MK, CK, NDK, and PPiase) (enzymes), 2.5 μL PURExpress Solution III (ribosomes), 1 μL RNase inhibitor, 150 ng of EGFP DNA template, 1.7 μL HEPES (pH 8.2, 1.5 M), and 20 μL of sample solution were mixed on ice. Nuclease-free water was added to bring the reaction volume to 50 μL. EGFP linear DNA template was amplified from gBlock encoding EGFP by Phusion High-Fidelity DNA Polymerase. Sample solutions are the reaction mixture of the AAA_P cycle after applying electricity for 5 h and the reaction mixture of the AAA_P cycle without AOR_{Aa} after applying electricity for 5 h (the negative control).

The reactions were gently mixed, transferred into a 384-well black transparent bottom plate, sealed to avoid evaporation, spun down at 2,000 rcf, 4°C in Thermo Fisher Scientific Heraeus Multifuge X1R Centrifuge, and incubated at 37°C for 6 h into Tecan Infinite M Plex plate reader. The plate reader parameters were the following: mode = fluorescence bottom reading, interval time = 2 min, λ_{exc} = 488 nm, λ_{em} = 515 nm, gain = 100, number of flashes = 25, integration time = 20 μs, shaking orbital duration = 20 s, and shaking orbital amplitude = 5.5 mm.

Coupling the AAA_P cycle with TX-TL for NanoLuc luciferase production

3.4 μL of solutionA(-Salts-tRNAs-AAs-ATP), 1.6 μL of salts solution, 2.5 μL of tRNAs solution, 2.5 μL of AAs solution, 1.25 μL custom PURExpress Solution II Δ(MK, CK, NDK, and PPiase) (enzymes), 1.25 μL PURExpress Solution III (ribosomes), 0.5 μL RNase inhibitor, 75 ng of pME-NanoLuc, 0.85 μL HEPES (pH 8.2, 1.5 M), and 10 μL of sample solution were mixed on ice. Nuclease-free water was added to bring the reaction volume to 25 μL. Sample solutions are the reaction mixture of the AAA_P cycle after applying electricity for 5 h and the reaction mixture of the AAA_P cycle without AOR_{Aa} after applying electricity for 5 h (the negative control).

The reactions were gently mixed and incubated at 37°C, for 6 h into the Thermo Fisher Scientific ProFlex PCR System. 200 μL luciferase assay reagent was prepared by mixing 1/50 v/v luciferase assay substrate:luciferase assay buffer. The reactions were diluted 1/1 v/v reaction:luciferase assay reagent and transferred into a 384-well white

transparent bottom plate. The plate reader parameters were the following: mode = luminescence, attenuation = none, and integration time = 1,000 ms.

SUPPLEMENTAL INFORMATION

Supplemental information can be found online at https://doi.org/10.1016/j.joule.2023.07.012.

ACKNOWLEDGMENTS

This work was supported by the Max Planck Society and the Fraunhofer-Gesellschaft in the framework of the MPG-FhG project eBioCO2n. S.G. was supported by an EMBO postdoctoral fellowship, and S.C.-B. was supported by the Green Talent Program of the German Federal Ministry of Education and Research (BMBF). We thank L. Brenker for providing plasmid p3WJdB; R. Inckemann for plasmid pME-NanoLuc; and J. Zarzycki, A. Pandi, and H. He for scientific discussions. Graphical abstract and Figures 1 and 3 were created with Biorender.com.

AUTHOR CONTRIBUTIONS

S.L. and T.J.E. conceived the project. S.L. designed the AAA cycle. S.L. designed and performed most of the experiments and analyzed the data. D.A. and S.C.-B. set up and optimized electrochemical systems. S.G. designed and performed TX-TL experiments. S.B. designed and performed TX experiments. N.P. performed mass spectrometry. D.H., F.A., and J.H. expressed and purified AOR. L.C.-L. synthesized HMV. M.K. assisted in protein purifications and enzyme kinetic assays. S.L. and T.J.E. wrote the manuscript with contributions from all authors.

DECLARATION OF INTERESTS

S.L., T.J.E., and J.H. have filed a patent covering the AAA cycle.

INCLUSION AND DIVERSITY

We support inclusive, diverse, and equitable conduct of research.

Received: January 11, 2023
Revised: May 23, 2023
Accepted: July 12, 2023
Published: August 16, 2023

REFERENCES

1. BP (2022). BP Statistical Review of World Energy 2022, p. 50. https://www.bp.com/content/dam/bp/business-sites/en/global/corporate/pdfs/energy-economics/statistical-review/bp-stats-review-2022-full-report.pdf.

2. Jones, D. (2022). Global electricity review 2022, p. 23. https://ember-climate.org/insights/research/global-electricity-review-2022/.

3. Steger, U., Achterberg, W., Blok, K., Bode, H., Frenz, W., Kost, M., Gather, C., Hanekamp, G., Kurz, R., and Imboden, D. (2005). Sustainable Development and Innovation in the Energy Sector (Springer Science & Business Media).

4. Salimijazi, F., Parra, E., and Barstow, B. (2019). Electrical energy storage with engineered biological systems. J. Biol. Eng. *13*, 38. https://doi.org/10.1186/s13036-019-0162-7.

5. Dodón, A., Quintero, V., Austin, M.C., and Mora, D. (2021). Bio-inspired electricity storage alternatives to support massive demand-side energy generation: a review of applications at building scale. Biomimetics (Basel) *6*, 51. https://doi.org/10.3390/biomimetics6030051.

6. De Luna, P., Hahn, C., Higgins, D., Jaffer, S.A., Jaramillo, T.F., and Sargent, E.H. (2019). What would it take for renewably powered electrosynthesis to displace petrochemical processes? Science *364*, eaav3506. https://doi.org/10.1126/science.aav3506.

7. Yishai, O., Lindner, S.N., Gonzalez de la Cruz, J., Tenenboim, H., and Bar-Even, A. (2016). The formate bio-economy. Curr. Opin. Chem. Biol. *35*, 1–9. https://doi.org/10.1016/j.cbpa.2016.07.005.

8. Claassens, N.J., Cotton, C.A.R., Kopljar, D., and Bar-Even, A. (2019). Making quantitative sense of electromicrobial production. Nat. Catal. *2*, 437–447. https://doi.org/10.1038/s41929-019-0272-0.

9. Li, H., Opgenorth, P.H., Wernick, D.G., Rogers, S., Wu, T.-Y., Higashide, W., Malati, P., Huo, Y.-X., Cho, K.M., and Liao, J.C. (2012). Integrated electromicrobial conversion of CO2 to higher alcohols. Science *335*, 1596. https://doi.org/10.1126/science.1217643.

10. Liu, C., Colón, B.C., Ziesack, M., Silver, P.A., and Nocera, D.G. (2016). Water splitting–biosynthetic system with CO2 reduction efficiencies exceeding photosynthesis. Science *352*, 1210–1213. https://doi.org/10.1126/science.aaf5039.

11. Nangle, S.N., Ziesack, M., Buckley, S., Trivedi, D., Loh, D.M., Nocera, D.G., and Silver, P.A. (2020). Valorization of CO2 through lithoautotrophic production of sustainable

chemicals in Cupriavidus necator. Metab. Eng. *62*, 207–220. https://doi.org/10.1016/j.ymben.2020.09.002.

12. Zheng, T., Zhang, M., Wu, L., Guo, S., Liu, X., Zhao, J., Xue, W., Li, J., Liu, C., Li, X., et al. (2022). Upcycling CO2 into energy-rich long-chain compounds via electrochemical and metabolic engineering. Nat. Catal. *5*, 388–396. https://doi.org/10.1038/s41929-022-00775-6.

13. Haas, T., Krause, R., Weber, R., Demler, M., and Schmid, G. (2018). Technical photosynthesis involving CO2 electrolysis and fermentation. Nat. Catal. *1*, 32–39. https://doi.org/10.1038/s41929-017-0005-1.

14. Nevin, K.P., Woodard, T.L., Franks, A.E., Summers, Z.M., and Lovley, D.R. (2010). Microbial electrosynthesis: feeding microbes electricity to convert carbon dioxide and water to multicarbon extracellular organic compounds. mBio *1*. e00103–e00110. https://doi.org/10.1128/mBio.00103-10.

15. Lu, S., Guan, X., and Liu, C. (2020). Electricity-powered artificial root nodule. Nat. Commun. *11*, 1505.

16. Rollin, J.A., Tam, T.K., and Zhang, Y.-H.P. (2013). New biotechnology paradigm: cell-free biosystems for biomanufacturing. Green Chem. *15*, 1708–1719. https://doi.org/10.1039/c3gc40625c.

17. Castañeda-Losada, L., Adam, D., Paczia, N., Buesen, D., Steffler, F., Sieber, V., Erb, T.J., Richter, M., and Plumeré, N. (2021). Bioelectrocatalytic cofactor regeneration coupled to CO2 fixation in a redox-active hydrogel for stereoselective C−C bond formation. Angew. Chem. Int. Ed. Engl. *60*, 21056–21061. https://doi.org/10.1002/anie.202103634.

18. Li, B., Steindel, P., Haddad, N., and Elliott, S.J. (2021). Maximizing (electro)catalytic CO2 reduction with a ferredoxin-based reduction potential gradient. ACS Catal. *11*, 4009–4023. https://doi.org/10.1021/acscatal.1c00092.

19. Lee, K.Y., Park, S.J., Lee, K.A., Kim, S.H., Kim, H., Meroz, Y., Mahadevan, L., Jung, K.H., Ahn, T.K., Parker, K.K., et al. (2018). Photosynthetic artificial organelles sustain and control ATP-dependent reactions in a protocellular system. Nat. Biotechnol. *36*, 530–535. https://doi.org/10.1038/nbt.4140.

20. Berhanu, S., Ueda, T., and Kuruma, Y. (2019). Artificial photosynthetic cell producing energy for protein synthesis. Nat. Commun. *10*, 1325. https://doi.org/10.1038/s41467-019-09147-4.

21. Biner, O., Fedor, J.G., Yin, Z., and Hirst, J. (2020). Bottom-up construction of a minimal system for cellular respiration and energy regeneration. ACS Synth. Biol. *9*, 1450–1459. https://doi.org/10.1021/acssynbio.0c00110.

22. Gutiérrez-Sanz, Ó., Natale, P., Márquez, I., Marques, M.C., Zacarias, S., Pita, M., Pereira, I.A., López-Montero, I., De Lacey, A.L., and Vélez, M. (2016). H2-fueled ATP synthesis on an electrode: mimicking cellular respiration. Angew. Chem. Int. Ed. Engl. *55*, 6216–6220. https://doi.org/10.1002/anie.201600752.

23. Folch, P.L., Bisschops, M.M.M., and Weusthuis, R.A. (2021). Metabolic energy conservation for fermentative product formation. Microb. Biotechnol. *14*, 829–858. https://doi.org/10.1111/1751-7915.13746.

24. Nissen, L.S., and Basen, M. (2019). The emerging role of aldehyde:ferredoxin oxidoreductases in microbially-catalyzed alcohol production. J. Biotechnol. *306*, 105–117. https://doi.org/10.1016/j.jbiotec.2019.09.005.

25. Seelmann, C.S., Willistein, M., Heider, J., and Boll, M. (2020). Tungstoenzymes: occurrence, catalytic diversity and cofactor synthesis. Inorganics *8*, 44. https://doi.org/10.3390/INORGANICS8080044.

26. White, H., Strobl, G., Feicht, R., and Simon, H. (1989). Carboxylic acid reductase: a new tungsten enzyme catalyses the reduction of non-activated carboxylic acids to aldehydes. Eur. J. Biochem. *184*, 89–96. https://doi.org/10.1111/j.1432-1033.1989.tb14993.x.

27. Heider, J., Ma, K., and Adams, M.W.W. (1995). Purification, characterization, and metabolic function of tungsten-containing aldehyde ferredoxin oxidoreductase from the hyperthermophilic and proteolytic archaeon Thermococcus strain ES-1. J. Bacteriol. *177*, 4757–4764. https://doi.org/10.1128/jb.177.16.4757-4764.1995.

28. Liew, F., Henstra, A.M., Köpke, M., Winzer, K., Simpson, S.D., and Minton, N.P. (2017). Metabolic engineering of Clostridium autoethanogenum for selective alcohol production. Metab. Eng. *40*, 104–114. https://doi.org/10.1016/j.ymben.2017.01.007.

29. Basen, M., Schut, G.J., Nguyen, D.M., Lipscomb, G.L., Benn, R.A., Prybol, C.J., Vaccaro, B.J., Poole, F.L., Kelly, R.M., and Adams, M.W.W. (2014). Single gene insertion drives bioalcohol production by a thermophilic archaeon. Proc. Natl. Acad. Sci. USA *111*, 17618–17623. https://doi.org/10.1073/pnas.1413789111.

30. Huber, C., Caldeira, J., Jongejan, J.A., and Simon, H. (1994). Further characterization of two different, reversible aldehyde oxidoreductases from Clostridium formicoaceticum, one containing tungsten and the other molybdenum. Arch. Microbiol. *162*, 303–309. https://doi.org/10.1007/BF00263776.

31. Arndt, F., Schmitt, G., Winiarska, A., Saft, M., Seubert, A., Kahnt, J., and Heider, J. (2019). Characterization of an aldehyde oxidoreductase from the mesophilic bacterium Aromatoleum aromaticum EbN1, a member of a new subfamily of tungsten-containing enzymes. Front. Microbiol. *10*, 71. https://doi.org/10.3389/fmicb.2019.00071.

32. Winiarska, A., Hege, D., Gemmecker, Y., Kryściak-Czerwenka, J., Seubert, A., Heider, J., and Szaleniec, M. (2022). Tungsten enzyme using hydrogen as an electron donor to reduce carboxylic acids and NAD^+. ACS Catal. *12*, 8707–8717. https://doi.org/10.1021/acscatal.2c02147.

33. Zarzycki, J., Sutter, M., Cortina, N.S., Erb, T.J., and Kerfeld, C.A. (2017). In vitro characterization and concerted function of three core enzymes of a glycyl radical enzyme - associated bacterial microcompartment. Sci. Rep. *7*, 42757. https://doi.org/10.1038/srep42757.

34. Trudeau, D.L., Edlich-Muth, C., Zarzycki, J., Scheffen, M., Goldsmith, M., Khersonsky, O., Avizemer, Z., Fleishman, S.J., Cotton, C.A.R., Erb, T.J., et al. (2018). Design and in vitro realization of carbon-conserving photorespiration. Proc. Natl. Acad. Sci. USA *115*. E11455–E11464. https://doi.org/10.1073/pnas.1812605115.

35. Montero-Lomelí, M., and De Meis, L. (1992). Glucose 6-phosphate and hexokinase can be used as an ATP-regenerating system by the Ca2+-ATPase of sarcoplasmic reticulum. J. Biol. Chem. *267*, 1829–1833. https://doi.org/10.1016/s0021-9258(18)46021-8.

36. Jung, J.K., Alam, K.K., Verosloff, M.S., Capdevila, D.A., Desmau, M., Clauer, P.R., Lee, J.W., Nguyen, P.Q., Pastén, P.A., Matiasek, S.J., et al. (2020). Cell-free biosensors for rapid detection of water contaminants. Nat. Biotechnol. *38*, 1451–1459. https://doi.org/10.1038/s41587-020-0571-7.

37. Ruccolo, S., Brito, G., Christensen, M., Itoh, T., Mattern, K., Stone, K., Strotman, N.A., and Sun, A.C. (2022). Electrochemical recycling of adenosine triphosphate in biocatalytic reaction cascades. J. Am. Chem. Soc. *144*, 22582–22588. https://doi.org/10.1021/jacs.2c08955.

38. Huber, C., Skopan, H., Feicht, R., White, H., and Simon, H. (1995). Pterin cofactor, substrate specificity, and observations on the kinetics of the reversible tungsten-containing aldehyde oxidoreductase from Clostridium thermoaceticum: preparative reductions of a series of carboxylates to alcohols. Arch. Microbiol. *164*, 110–118. https://doi.org/10.1007/BF02525316.

39. Kuhns, M., Trifunović, D., Huber, H., and Müller, V. (2020). The Rnf complex is a Na+ coupled respiratory enzyme in a fermenting bacterium, Thermotoga maritima. Commun. Biol. *3*, 431. https://doi.org/10.1038/s42003-020-01158-y.

40. Buckel, W., and Thauer, R.K. (2018). Flavin-based electron bifurcation, ferredoxin, flavodoxin, and anaerobic respiration with protons (Ech) or NAD^+ (Rnf) as electron acceptors: A historical review. Front. Microbiol. *9*, 401. https://doi.org/10.3389/fmicb.2018.00401.

41. Shimizu, Y., Kanamori, T., and Ueda, T. (2005). Protein synthesis by pure translation systems. Methods *36*, 299–304. https://doi.org/10.1016/j.ymeth.2005.04.006.